Published in final edited form as:
Comp Biochem Physiol Part D Genomics Proteomics. 2009 March ; 4(1): 21–31. doi:10.1016/j.cbd.2008.09.003.

Proteomic Analysis of Anoxia Tolerance in the Developing Zebrafish Embryo

Bryce A. Mendelsohn[a], **James P. Malone**[b], **R. Reid Townsend**[b,c], and **Jonathan D. Gitlin**[a]

[a] Department of Pediatrics, Washington University School of Medicine, St. Louis, Missouri 63110, USA

[b] Department of Medicine, Washington University School of Medicine, St. Louis, Missouri 63110, USA

[c] Departments of Cell Biology and Physiology, Washington University School of Medicine, St. Louis, Missouri 63110, USA

Abstract

While some species and tissue types are injured by oxygen deprivation, anoxia tolerant organisms display a protective response that has not been fully elucidated and is well-suited to genomic and proteomic analysis. However, such methodologies have focused on transcriptional responses, prolonged anoxia, or have used cultured cells or isolated tissues. In this study of intact zebrafish embryos, a species capable of >24 h survival in anoxia, we have utilized 2D difference in gel electrophoresis to identify changes in the proteomic profile caused by near-lethal anoxic durations as well as acute anoxia (1 h), a timeframe relevant to ischemic events in human disease when response mechanisms are largely limited to post-transcriptional and post-translational processes. We observed a general stabilization of the proteome in anoxia. Proteins involved in oxidative phosphorylation, antioxidant defense, transcription, and translation changed over this time period. Among the largest proteomic alterations was that of muscle cofilin 2, implicating the regulation of the cytoskeleton and actin assembly in the adaptation to acute anoxia. These studies in an intact embryo highlight proteomic components of an adaptive response to anoxia in a model organism amenable to genetic analysis to permit further mechanistic insight into the phenomenon of anoxia tolerance.

Keywords

Anoxia; proteomic; zebrafish

1. Introduction

Understanding cellular and organismal responses to the energetic challenges posed by anoxia may permit insight into ischemic disease as well as the metabolic perturbations that occur in conditions such as cancer (Bui et al. 2006; Bickler et al. 2007). Broad and unbiased approaches examining global changes in gene expression and activity offer an opportunity to uncover

Corresponding Author: Jonathan D. Gitlin, M.D., Edward Mallinckrodt Department of Pediatrics, Washington University School of Medicine, 660 South Euclid Avenue, Box 8208, St. Louis, Missouri 63110, USA, Phone: (314) 286-2764; Fax: (314) 286-2784, Email: jonathan.d.gitlin@vanderbilt.edu.

critical signals and responses to limited oxygen availability. These studies are of particular interest in anoxia tolerant organisms as the processes identified may represent protective adaptations with therapeutic implications. The zebrafish embryo (*Danio rerio*) has been demonstrated to survive over 24 h in anoxia (Padilla et al. 2001; Mendelsohn et al. 2008b), and the accessibility of this organism to forward and reverse genetic and pharmacologic analysis as well as its rapid transparent development make it an excellent model with which to study the mechanisms of anoxia tolerance.

Acute anoxia has the potential to cause significant perturbations in cellular energy homeostasis before new genes can be transcribed and translated. Furthermore, new gene expression is energy-demanding (Hochachka et al. 1996). Thus, an early component of the sensation and response to anoxia may include post-transcriptional or post-translational mechanisms. Consistent with this idea, recent studies have revealed that chemical anoxia caused by cyanide caused an almost immediate developmental arrest in zebrafish embryos that was reversible when the drug was removed (Mendelsohn et al. 2008b). Critically, arrest occurred despite the inhibition of transcription (Mendelsohn et al. 2008a). This rapid, transcription-independent response may preclude pathways that require new gene expression and suggests that the adaptive response to anoxia is mediated at least in part by activities of the existing pool of mRNA and protein. Proteomic analysis is ideally suited to study these early changes in anoxia.

Previous proteomic studies have examined nuclear (Shakib et al. 2005), skeletal muscle (De Palma et al. 2007), or hippocampal proteins (Klein et al. 2003) regulated by prolonged hypoxia. These studies have implicated a broad range of cellular functions in the response to hypoxia, including metabolic enzymes and hypoxia-inducible factor (HIF) targets. Recently, methodologies for proteomic analysis of zebrafish have been developed (Link et al. 2006b; Tay et al. 2006). Proteomic techniques in zebrafish have been utilized to observe changes in the proteome over developmental time (Lucitt et al. 2008) or in different germ layers (Link et al. 2006a), and one study has investigated proteomic changes in zebrafish muscle after prolonged hypoxia, though proteins were not identified (Bosworth et al. 2005). Additional studies have examined the effects of long term anoxia in rainbow trout cells (Wulff et al. 2008b) and compared the impact of anoxia and azide treatment following reoxygenation (Wulff et al. 2008a), though these experiments did not utilize an intact organism and did not examine proteomic changes immediately following acute anoxia. Nevertheless, these important studies have laid the groundwork for the analysis of the proteomic responses to environmental stressors in a teleost model organism.

In this current study we applied 2D difference in gel electrophoresis (2D-DIGE) to examine the response of zebrafish embryos to anoxia with particular focus on the earliest responses to acute anoxia (1 h). We have also assessed the stability of the proteome as an arrested embryo nears its maximum duration of anoxic viability. Broadly, though the proteome is globally stabilized even after prolonged anoxia, modifications of the proteome caused by anoxia involved proteins regulating translation, transcription, oxidative phosphorylation and the cytoskeleton. Several proteins, including muscle cofilin 2, function to regulate actin assembly, suggesting a role for the cytoskeleton in the immediate and long term adaptation to anoxia.

2. Materials and Methods

2.1 Experimental Animals

Wild type (AB strain) zebrafish (*Danio rerio*, Cyprinidae, Cypriniformes)were maintained in a 14h-light/10h-dark cycle and housed according to guidelines of the Washington University Animal Studies Committee. Embryos were obtained by *in vitro* fertilization to maximize developmental synchronization and in all conditions were incubated at 28.5° C. Images were taken with an SZX12 zoom stereomicroscope (Olympus).

2.2 Environmental conditions

Normoxia is defined as egg water equilibrated with room air consisting of an approximate 78:20 ratio of nitrogen and oxygen, water vapor and trace carbon dioxide. A Bactron II anaerobic chamber (Shel Labs, Cornelius, OR, USA) was used to create an anoxic environment and contains an atmosphere of 90% N_2, 5% CO_2, and 5% H_2 and a temperature-controlled incubator. A palladium catalyst, which removes residual oxygen by reaction with H_2, was heated to above 160° C to reactivate it and was replaced daily. To account for potential acidification of egg water by CO_2, all egg water was buffered with 1 mg/mL sodium bicarbonate, pH 7.1. No developmental abnormalities were observed in this egg water, the stability of the pH of this egg water was verified in normoxia and anoxia, and it was used in both normoxic and anoxic experiments. Incubation of embryos in 5% CO_2 plus room air in buffered egg water did not alter the rate or morphology of development.

2.3 Sample preparation

Previous studies utilizing zebrafish have noted that removal of the yolk facilitates proteomic analysis (Link et al. 2006b). Twenty-four hours post fertilization (hpf) represents a time point when embryos are young enough such that they are robustly anoxia tolerant (capable of >24 h survival in anoxia) and old enough that the yolk can be readily removed. Therefore the following experiments were carried out at this developmental stage. Embryos were rapidly cooled on ice, manually dechorionated and deyolked, and stored at −80° C.

2.4 Two dimensional difference gel electrophoresis (2D-DIGE)

Solubilized zebrafish samples were labeled with charge-matched cyanine dyes as described previously (Ünlü et al. 1997; Tonge et al. 2001). Zebrafish protein (50 μg) was prepared in sample buffer (30 mM Tris-HCl pH 8.5, 7 M urea, 2 M thiourea, 4% CHAPS) and labeled with 400 pmol of Cy2, Cy3 or Cy5. Pools were prepared by mixing equal protein amounts of each zebrafish embryo sample following labeling by the above method. All samples were ultimately equilibrated into immobilized pH gradient (IPG) strips under 100 V followed by isoelectric focusing using a maximum of 10,000 focusing volts (PROTEAN IEF cell – BioRad). After focusing, proteins were reduced with TCEP (10 mM) and alkylated with iodoacetamide (20 mM). The IPG strip was then layered on a 10% polyacrylamide gels followed by SDS-PAGE separation. Samples were imaged with a Typhoon Imager (GE Healthcare) using specific excitation/emission wavelengths: 488/520 nm for Cy2, 520/580 nm for Cy3, 620/670 nm for Cy5.

2.5 Image analyses (2D-DIGE), mass spectrometry and protein identification

The DeCyder (v. 6.5) software tools (GE Healthcare) were used for image analysis. The DIA (differential in-gel analysis) module was used to align and normalize images within each gel. Spots with slopes > 1.1, areas < 100, volumes < 10,000 and peak heights < 100 were excluded. The DIA module calculated abundance ratios using a normalization algorithm that was applied as previously described (Alban et al. 2003). For comparative pair-wise analyses of gel features across different physical gels, the DIA data sets were analyzed using the BVA (biological variation analysis) module. Spot volumes were converted to ratios of a pooled internal standard (24 hpf normoxic). Using the EDA (Extended Data Analysis) module, a t-test was performed to determine the statistical significance of Normoxic/Anoxic ratios for each gel feature. Unsupervised hierarchical clustering was used to identify gel features which were statistically important in the differentiation of normoxic and anoxic growth environments. Spots were excised robotically (ProPic, Genomic Solutions) using a triangulation algorithm implemented with in-house software. The gel pieces were digested *in situ* with trypsin (Hăvlis et al. 2003). Samples were processed and analyzed using nano-reversed-phase HPLC interfaced to either an electrospray-quadrupole-time-of-flight mass spectrometer (Q-STAR-XL, Applied

Biosystems) (King et al. 2006) or an electrospray-linear ion trap-Fourier transform ion cyclotron mass spectrometer (LTQ-FT, Thermo-Finnigan) (King et al. 2007) and operated as previously described, respectively. The MS and MS/MS data from the nano-LC-FTMS/MS were collected in the profile mode. The "raw" files were processed using MASCOT Distiller, version 2.1.1.0 (Matrix Science, Oxford, U.K.) with the following settings: 1) MS processing: 200 data points per Da; no aggregation method; maximum charge state = +8; minimum number of peaks = 1. 2) MS/MS processing: 200 data points per Da; time domain aggregation method enabled; minimum number of peaks = 10; precursor charge and *m/z*, try to re-determine from the survey scan (tolerance = 2.5 Da); charge defaults = +2/+3; maximum charge state = +2. 3) Time domain parameters: minimum precursor mass = 700; maximum precursor mass =16,000; precursor *m/z* tolerance for grouping =0.1; maximum number of intermediate scans = 5; minimum number of scans in a group = 1. 4) Peak Picking: maximum iterations = 500; correlation threshold = 0.90; minimum signal-to-noise = 3; minimum peak *m/z* = 50; maximum peak *m/z* = 100,000; minimum peak width = 0.001; maximum peak width = 2; and expected peak width = 0.01. The resulting Mascot generic files (.mgf) were exported to MASCOT, version 2.1.6. The tandem MS data from the LTQ-FT were searched against National Center for Biotechnology Information non-redundant databases that were downloaded on 2007-02-18 with the following constraints: MS tolerance = 10 ppm, MS/MS tolerance = 0.8 Da with fixed modifications of cysteine residues (carbamidomethylation) and variable oxidation of methionine residues. The tandem MS data from the QSTAR-XL were searched with an MS and MS/MS tolerance of 1 Da and 0.2 Da, respectively, and the modifications as above. The resulting DAT files were imported into Scaffold, ver. 2.0 (Proteome Software, Portland, OR) to identify proteins with > 95% confidence and to determine the spectral counts for each protein.

2.6 Pathway Analysis

The pathway analysis was generated using Ingenuity Pathways Analysis software, version 6.3 (Ingenuity® Systems, www.ingenuity.com). Peptides from all experiments were searched as described above and all identified proteins with a MASCOT score >40 were imported into Ingenuity for analysis.

3. Results

3.1. Analysis of proteomic profiles of zebrafish embryos before and after acute anoxia

To study the proteomic impact of acute anoxia, we obtained samples from 3 experimental conditions for analysis by 2D-DIGE: 1) zebrafish embryos at 24 h post fertilization (hpf) to determine the proteomic profile prior to exposure to anoxia, 2) embryos incubated under anoxic conditions for 1 h beginning at 24 hpf and 3) embryos that remained in normoxia for 1 additional h beginning at 24 hpf to account for normal developmental changes occurring between 24 and 25 hpf. These three samples were run in the same 2D gel as described in *Materials and Methods* for comparative image analysis of proteomic profiles from these conditions (Gel 1, Fig. S1). This initial study focused on analyzing the largest differences between the anoxic and normoxic samples. Importantly, 95% of proteins changed less than 1.51-fold from 24 hpf +1 h normoxia compared to 24 hpf +1 h anoxia. Twenty-four spots were subjected to *in situ* gel digestion and tandem mass spectrometry. Unique proteins identified (Table 1) were categorized as 1) cytoskeletal proteins, 2) translation regulators, 3) keratins, 4) vitellogenins, 5) antioxidant proteins, and 6) other proteins. The results from mass spectrometry and database searching are given in Table S1.

3.2. Analysis of proteomic profiles of zebrafish embryos before and after prolonged anoxia

Prolonged periods of anoxia provide an opportunity to study additional proteomic changes permitting the survival of zebrafish embryos in anoxia such as the induction of new gene expression and to assess the stability of the proteome as the embryo approaches the limit of its

capacity for anoxic survival. Interestingly, compared to normoxic embryos (Fig. 1A), prolonged anoxia (24 h) caused embryos to appear markedly opaque and granular (Fig. 1B). Furthermore, embryos anoxic for 24 h were more rigid to the touch and the yolk sac was more brittle compared to normoxic embryos, a property that also became more pronounced with longer durations of anoxic exposure. These alterations in appearance were reversed when anoxic embryos were returned to normoxia (data not shown). Because previous studies have determined that 24 hpf zebrafish embryos are not capable of surviving in anoxia for durations longer than approximately 28 h (Mendelsohn et al. 2008b), combined with the increasing opacity and rigidity described above, we hypothesized that zebrafish embryos nearing the limit of their viability in anoxia may display substantial degenerative alterations to the proteome.

To examine this possibility, we compared the proteomic profiles of 24 hpf embryos with 24 hpf +24 h in anoxia. This experiment was conducted twice, and the third sample varied between these two repetitions. To observe proteomic changes that occurred during normal development, in Gel 2 we utilized embryos at 24 hpf +6 h normoxia as this third sample in one gel (Fig. S2), while in Gel 3 we utilized 24 hpf +24 h of normoxia (Fig. S3). Surprisingly, we observed minimal changes in the proteome following 24 h of anoxia (Fig. 1C), in which 95% of resolved spots changed <1.81-fold (Table 2). Twenty-four spots were picked, 14 of which were identified (58.3%). The majority of the proteins identified from the first experiment examining prolonged anoxia were vitellogenins (Table 3), components of the yolk sac. While these differences may reflect actual regulatory processes involving vitellogenins, it is also plausible that the altered consistency of the yolk sac in anoxic embryos, as described above, resulted in a different degree of yolk removal, thus causing an apparent change in the levels of yolk proteins. Nevertheless, this analysis identified several non-vitellogenin proteins as changing after prolonged anoxia (Table 3), notably the RNA polymerase II transcriptional coactivator PC4. This protein was identified in two spots at nearly exactly the same molecular weight but separated by isoelectic point (pI). As one of these spots increased in intensity while the other decreased, this shift may represent a change in posttranslational modification. From the second experiment examining prolonged anoxia (Gel 3) we selected 30 spots from different locations compared to the first experiment (Gel 2) and identified 20 (66.7%), including proteins involved in regulating translation and the cytoskeleton (Table 4).

3.3. Proteomic changes after acute anoxia using 2D-DIGE with an internal standard

Most of the proteomic changes observed in acute anoxia were of low magnitude, though responses that occur slowly or do not require a large change in protein level or regulation may represent important components of the effects of—or response to—anoxia. Therefore, to distinguish between experimental and biological variation, we used the multiplexing attribute of 2D-DIGE to perform an experiment with an internal standard sample to normalize the protein abundances across multiple gels (Alban et al. 2003). We performed 2D-DIGE on two additional independent experiments (Gels 4 and 5) of the same three experimental conditions utilized for the initial analysis of acute anoxia (Gel 1). These two experiments were analyzed in combination with the 1 h anoxic gel described above (Gel 1), and we conducted a “biological variation analysis” (BVA) of these 3 gels using the starting 24 hpf sample to normalize across gels (Fig. 2A). Analysis was restricted to spots that were visualized in all 3 gels and displayed statistically significant variation ($p<0.05$). With these criteria, 21 spots were identified that changed in intensity after 1 h in anoxia beginning at 24 hpf compared to 1 h in normoxia (Fig. 2B) corresponding to the spots on the 2D gel shown in Fig. 2C. These spots distinguished normoxic and acutely anoxic zebrafish embryos. Interestingly, all but one of these spots decreased in intensity.

To identify the proteins represented by gel features displaying altered intensity after acute anoxia these spots were picked and subjected to analysis by tandem mass spectroscopy.

Thirteen of these 21 spots (61.9%) were identified (Table 5), including eEF1A and muscle cofilin 2, which had been identified in our previous experiments as changing in acute (Table 1) and prolonged anoxia (Table 4). Additional proteins, including the mitochondrial ATP synthase F1 subunit and tropomyosin 3, were also observed to change in acute anoxia.

3.4. Changes in muscle cofilin 2 over different durations of anoxia

One of the largest changes in the proteomic profile caused by acute anoxia was the decrease in intensity of a spot containing muscle cofilin 2 (Fig. 3, Panels A–C). Importantly, this change decrease in intensity did not occur between 24 and 25 hpf in normoxia, revealing that the observed difference was not due to normal developmental processes but rather was specific for anoxia. To further examine the kinetics of the change in intensity of this cofilin spot we compared the cofilin fluorescent feature volumes at 1 h and 2 h of anoxic exposure. These studies revealed that while the intensity of this cofilin spot decreased during normal development between 24 and 48 hpf, the decline was even larger in anoxia (Fig. 3D–F), >10-fold. Furthermore, this relative decrease in intensity after 24 h of anoxia was greater than after 1 h of anoxia (−2.53 fold), revealing that anoxia-specific regulation of cofilin increased in magnitude with time in anoxia.

3.5. Changes in cofilin after CO_2 or cyanide exposure

Previous studies have revealed that developmental arrest in anoxic zebrafish is mediated by the inhibition of oxidative phosphorylation independent of the availability of molecular oxygen (Mendelsohn et al. 2008b). Therefore we obtained samples of 24 hpf normoxic embryos, 24 hpf embryos plus a 1 h incubation in 500 μM potassium cyanide (KCN) in normoxia, and, as an additional control, 24 hpf embryos incubated for 1 h in 5% CO_2 in normoxia, all at the same temperature. This analysis revealed that CO_2 did not mimic the effects of anoxia on cofilin (Fig. 3G and H). However, incubation in KCN recapitulated the reduction in intensity of the cofilin spot observed in anoxia (Fig. 3G and I), revealing that this alteration in the proteomic profile is likely due to a perturbation in energy homeostasis rather than the lack of molecular oxygen *per se* in anoxia.

3.6. Network analysis of cytoskeletal proteins identified by 2D-DIGE

Pathway analysis serves to connect individual genes or proteins identified in global surveys such as this one with more general networks based on interactions described in the literature, providing a broader perspective of the cellular systems and key regulators involved in the process of interest. To this end we analyzed all of the proteins identified by MS/MS in all experiments (Table S2) by mapping them to existing networks. One network generated by this approach (Fig. 4) included cofilin as well as additional proteins involved in actin dynamics, revealing that anoxia induced changes in several proteins that function to regulate the actin cytoskeleton. Interestingly, the actin network connected via elongation factor 2 to several proteins that regulate translation, suggesting that the regulation of translation is also an important component of the response to anoxia and may be connected to the activity of the cytoskeleton (see *Discussion*). This type of pathway analysis thus implicates and connects networks in an anoxia tolerant organism and generates new hypotheses whose biological significance can now be experimentally validated.

4. Discussion

Proteomic alterations induced by anoxia are of unique interest in an organism capable of anoxic survival as such changes are more likely to represent protective biochemical adaptations than those observed in anoxia sensitive organisms and may provide insight into ischemic and metabolic perturbations in disease states. We have studied the effects of acute anoxia to observe proteomic changes that do not depend on new gene expression and thus represent post-

transcriptional and post-translational changes. We have also compared the proteomic profiles of zebrafish embryos in normoxia and following prolonged anoxia, revealing a generally stable proteome with alterations that provide insight into the adaptation to anoxia.

Several important experimental assumptions of this study bear discussion. We have utilized an entire organism in these proteomic analyses, making it possible to identify changes that occur in any tissue or cell type. Using an intact organism also permits identification of proteins that connect or signal between cells that might not be expressed in isolated tissues or in culture. However, it is possible that this approach might obscure other important changes restricted to a minority cell type, and further analysis is necessary to determine the relevant cell type in which any observed changes occurred. Another important consideration involves the interpretation of the direction of change in each spot. Though individual spots are characterized as either increasing or decreasing, the complexity of potential causes for such observed changes, including altered expression level, proteolytic cleavage and posttranslational modification, confound any direct conclusion of higher or lower activity based on spot intensity. Rather, without further analysis, variations in spot intensity can only be generally interpreted as a change in protein regulation.

An important conclusion from this work is that acute or prolonged arrest in anoxia tolerant zebrafish embryos is associated with a stabilized proteome that is neither abundantly degraded nor extensively posttranslationally modified. Numerous processes in development require short-lived intra- and extra-cellular molecules such as morphogens that direct development and might be expected to degrade during arrest. It is possible that such proteins were below the threshold of detection of the methodologies used in this study. Nevertheless, it may be more adaptive for arrest to occur via means other than the degradation of growth and patterning signals so that development can resume properly when oxygen is restored. Future studies of the proteomic profile of embryos after lethal durations of anoxia that cause poor recovery may elucidate the critical cellular and organismal functions that eventually fail in anoxia.

Several proteins identified in this study function to regulate the energy consuming processes of transcription and translation. Transcriptional coactivator PC4 has been shown to bind DNA and inhibit transcription in its unphosphorylated state, and phosphorylation of PC4 has therefore been hypothesized to release this inhibition and serve as a critical regulatory step in transcription (Malik et al. 1998). The observed change in pI in our experiments is consistent with a model in which PC4 becomes dephosphorylated, reverting to a state in which transcription is repressed, perhaps acting as an energy sensor to regulate transcription while allowing assembled transcription factors to remain in place in anticipation of the return of oxygen. The levels of eukaryotic elongation factor 1a (eEF1A), a central component of the translational machinery, were observed to change in both acute and prolonged anoxia (Tables 1, 4 and 5). This protein has been implicated in the response to limited oxygen and has been demonstrated to associate abnormally with polysomes during hypoxia and low pH and may mediate the initial inhibition of protein synthesis (Vayda et al. 1995). eEF1A has been observed to change in hypoxic cells in other microarray (Scandurro et al. 2001) and proteomic (Son et al. 2008) analyses. Furthermore, reduced eEF1A levels have been shown to protect against hydrogen peroxide-induced (Chen et al. 2000) and lipotoxicity-induced apoptosis (Borradaile et al. 2006), perhaps suggesting that zebrafish avoid cell death in anoxia in part by the regulation of eEF1A. Our initial study of acute anoxia also detected a change in elongation factor 2 (Table 1), which has also been implicated in regulating translation during hypoxia by receiving signals from AMP-activated protein kinase (Horman et al. 2002) and the Target of Rapamycin (Connolly et al. 2006). Anoxic inhibition of transcription and translation is consistent with the dearth of proteins observed to increase in abundance during anoxia and may function to conserve energy.

The alpha subunit of the F1 mitochondrial ATP synthase was observed to change in acute anoxia (Table 4), a protein critical for maintaining energy homeostasis (Das 2003). When the mitochondrial proton motive force begins to collapse in anoxia the ATP synthase can operate in reverse, consuming ATP by pumping protons into the inner membrane space (St-Pierre et al. 2000). Biochemical observations have demonstrated that the activity of this protein is inhibited in anoxia such that less ATP hydrolysis occurs than would be predicted (Das et al. 1990;St-Pierre et al. 2000). Our observations here indicate that the mechanism of this regulation may involve the direct degradation and/or modification of the ATP synthase itself.

One of the largest changes in level or regulation following acute or prolonged anoxia was that of muscle cofilin 2. This protein has not been previously identified in global studies of anoxia or hypoxia responsive genes, though changes in cofilin 2 have been observed in the setting of ischemia (Schwartz et al. 1999) or oxidative stress (Lee et al. 2006). Cofilins are activated by dephosphorylation as well as other mechanisms (van Rheenen et al. 2007) and regulate the turnover, assembly and monomer nucleotide exchange of actin filaments (Suurna et al. 2006). Importantly, activation of cofilin has been demonstrated to regulate the actin cytoskeleton during ischemia and cofilin-mediated actin rod formation has been observed to support ATP homeostasis and improve mitochondrial membrane potential during ATP depletion (Bernstein et al. 2006; Suurna et al. 2006). As cofilin 2 is predominantly expressed in muscle (Thisse and Thisse, 2004), this response may be specific to the adaptation of muscle or may occur via other related proteins in non-muscle tissues.

Tropomyosin was also observed to change in acute anoxia. Intriguingly, this cytoskeletal component functions to stabilize actin filaments, opposing the action of cofilin. The balance of tropomyosin and cofilin is critical for regulating actin assembly *in vivo* (Cooper 2002; Ono et al. 2002), and the observation that both proteins changed in acute anoxia further supports a model in which the regulation of actin dynamics contribute to an early response to anoxia. Strikingly, in addition to its role in translation, eEF1A also possesses actin binding properties and may crosslink actin filaments (Owen et al. 1992), and mutations in eEF1A cause cytoskeletal abnormalities (Gross et al. 2007). This dual role for eEF1A has been proposed to function as a link between translation and cytoskeletal dynamics (Gross et al. 2007), and is consistent with a connection between the cytoskeleton and translation as suggested by Figure 4. Taken together, our observation that several actin binding proteins with roles in regulating actin assembly and stability are differentially regulated in acute anoxia suggests that the response of the cytoskeleton represents an important component of the adaptation to acute anoxia in the zebrafish embryo and perhaps in other organisms as well. The regulation of the actin cytoskeleton may underlie the gel-like appearance and physical properties of arrested embryos and might function to stabilize micro- and macroscopic embryonic structures during a prolonged arrest.

Previous studies have demonstrated that KCN as well as other inhibitors of oxidative phosphorylation cause a developmental arrest similar to that observed in anoxia (Mendelsohn et al. 2008b). The observation that KCN treatment in normoxia caused an acute change in the cofilin spot (Fig. 3G and I) provides further evidence that the molecular response to anoxia is fundamentally a response to the loss of energy produced via oxidative phosphorylation. The consistent, rapid change of this spot in anoxia and cyanide also supports the concept that post-translational pathways may be at least in part responsible for causing arrest.

The process of elucidating the molecular mechanisms underlying the physiologic adaptations of anoxia tolerant organisms may be greatly assisted by new technologies that provide a comprehensive view of gene activity during an environmental stress (Storey 2006). These observations identify molecular pathways which can then be manipulated in the model organism as the foundation for future studies. Our findings suggest several pathways that may

contribute to the viable arrest observed in anoxic zebrafish embryos, such as the regulation of actin dynamics and translation (Fig. 4). Of importance to the future study of these pathways, zebrafish embryos transition away from anoxia tolerance during embryogenesis. Therefore, in addition to identifying anoxia-induced changes in the zebrafish embryo proteome, these studies now allow detailed comparative analyses of the proteomic responses of anoxia tolerant and sensitive stages of zebrafish development and among specific cell types. Performing these proteomic studies in the zebrafish embryo, a model amenable to forward and reverse genetic and pharmacologic analysis, permits the *in vivo* examination of gene products identified from this and future proteomic approaches, offering novel insight into the mechanisms of oxygen and energy sensing, developmental arrest, and metabolic reprogramming.

Supplementary Material

Refer to Web version on PubMed Central for supplementary material.

Acknowledgments

We thank Petra Gilmore, Alan Davis and Marjorie Case for providing excellent technical assistance for the proteomic studies, and Amy Koerber for zebrafish husbandry. This work was supported by the National Institutes of Health grants DK44464 (J.D.G.), P30-DK52574 (WU DDRCC), Medical Scientist Training Program Grant T32 GM07200 (B.A.M.), the Chancellor's Hartwell Prize for Innovative Research from Washington University (J.D.G.), and by the National Centers for Research Resources of the National Institutes of Health (Grant P41-RR00954), and by the W. M. Keck Foundation.

References

Alban A, David SO, Bjorkesten L, Andersson C, Sloge E, Lewis S, Currie I. A novel experimental design for comparative two-dimensional gel analysis: two-dimensional difference gel electrophoresis incorporating a pooled internal standard. Proteomics 2003;3:36–44. [PubMed: 12548632]

Bernstein BW, Chen H, Boyle JA, Bamburg JR. Formation of actin-ADF/cofilin rods transiently retards decline of mitochondrial potential and ATP in stressed neurons. Am J Physiol 2006;291:C828–839.

Bickler PE, Buck LT. Hypoxia tolerance in reptiles, amphibians, and fishes: life with variable oxygen availability. Annu Rev Physiol 2007;69:145–170. [PubMed: 17037980]

Borradaile NM, Buhman KK, Listenberger LL, Magee CJ, Morimoto ET, Ory DS, Schaffer JE. A critical role for eukaryotic elongation factor 1A-1 in lipotoxic cell death. Mol Biol Cell 2006;17:770–8. [PubMed: 16319173]

Bosworth, CAt; Chou, CW.; Cole, RB.; Rees, BB. Protein expression patterns in zebrafish skeletal muscle: initial characterization and the effects of hypoxic exposure. Proteomics 2005;5:1362–1371. [PubMed: 15732137]

Bui T, Thompson CB. Cancer's sweet tooth. Cancer Cell 2006;9:419–420. [PubMed: 16766260]

Chen E, Proestou G, Bourbeau D, Wang E. Rapid up-regulation of peptide elongation factor EF-1alpha protein levels is an immediate early event during oxidative stress-induced apoptosis. Exp Cell Res 2000;259:140–148. [PubMed: 10942586]

Connolly E, Braunstein S, Formenti S, Schneider RJ. Hypoxia inhibits protein synthesis through a 4E-BP1 and elongation factor 2 kinase pathway controlled by mTOR and uncoupled in breast cancer cells. Mol Cell Biol 2006;26:3955–3965. [PubMed: 16648488]

Cooper JA. Actin dynamics: tropomyosin provides stability. Curr Biol 2002;12:R523–525. [PubMed: 12176375]

Das AM. Regulation of the mitochondrial ATP-synthase in health and disease. Mol Genet Metab 2003;79:71–82. [PubMed: 12809636]

Das AM, Harris DA. Regulation of the mitochondrial ATP synthase in intact rat cardiomyocytes. Biochem J 1990;266:355–361. [PubMed: 2138454]

De Palma S, Ripamonti M, Vigano A, Moriggi M, Capitanio D, Samaja M, Milano G, Cerretelli P, Wait R, Gelfi C. Metabolic modulation induced by chronic hypoxia in rats using a comparative proteomic analysis of skeletal muscle tissue. J Proteome Res 2007;6:1974–1984. [PubMed: 17391017]

Gross SR, Kinzy TG. Improper organization of the actin cytoskeleton affects protein synthesis at initiation. Mol Cell Biol 2007;27:1974–1989. [PubMed: 17178834]

Hăvlis J, Thomas H, Sebela M, Shevchenko A. Fast-response proteomics by accelerated in-gel digestion of proteins. Anal Chem 2003;75:1300–1306. [PubMed: 12659189]

Hochachka PW, Buck LT, Doll CJ, Land SC. Unifying theory of hypoxia tolerance: molecular/metabolic defense and rescue mechanisms for surviving oxygen lack. Proc Natl Acad Sci USA 1996;93:9493–9498. [PubMed: 8790358]

Horman S, Browne G, Krause U, Patel J, Vertommen D, Bertrand L, Lavoinne A, Hue L, Proud C, Rider M. Activation of AMP-activated protein kinase leads to the phosphorylation of elongation factor 2 and an inhibition of protein synthesis. Curr Biol 2002;12:1419–1423. [PubMed: 12194824]

King JB, Gross J, Lovly CM, Piwnica-Worms H, Townsend RR. Identification of protein phosphorylation sites within Ser/Thr-rich cluster domains using site-directed mutagenesis and hybrid linear quadrupole ion trap Fourier transform ion cyclotron resonance mass spectrometry. Rapid Commun Mass Spectrom 2007;21:3443–3451. [PubMed: 17918214]

King JB, Gross J, Lovly CM, Rohrs H, Piwnica-Worms H, Townsend RR. Accurate mass-driven analysis for the characterization of protein phosphorylation. Study of the human Chk2 protein kinase. Anal Chem 2006;78:2171–2181. [PubMed: 16579595]

Klein JB, Gozal D, Pierce WM, Thongboonkerd V, Scherzer JA, Sachleben LR, Guo SZ, Cai J, Gozal E. Proteomic identification of a novel protein regulated in CA1 and CA3 hippocampal regions during intermittent hypoxia. Respir Physiol Neurobiol 2003;136:91–103. [PubMed: 12853002]

Lee CK, Park HJ, So HH, Kim HJ, Lee KS, Choi WS, Lee HM, Won KJ, Yoon TJ, Park TK, Kim B. Proteomic profiling and identification of cofilin responding to oxidative stress in vascular smooth muscle. Proteomics 2006;6:6455–75. [PubMed: 17099934]

Link V, Carvalho L, Castanon I, Stockinger P, Shevchenko A, Heisenberg CP. Identification of regulators of germ layer morphogenesis using proteomics in zebrafish. J Cell Sci 2006a;119:2073–2083. [PubMed: 16638810]

Link V, Shevchenko A, Heisenberg CP. Proteomics of early zebrafish embryos. BMC Dev Biol 2006b; 6:1. [PubMed: 16412219]

Lucitt MB, Price TS, Pizarro A, Wu W, Yocum AK, Seiler C, Pack MA, Blair IA, Fitzgerald GA, Grosser T. Analysis of the zebrafish proteome during embryonic development. Mol Cell Proteomics. 2008

Malik S, Guermah M, Roeder RG. A dynamic model for PC4 coactivator function in RNA polymerase II transcription. Proc Natl Acad Sci USA 1998;95:2192–2197. [PubMed: 9482861]

Mendelsohn BA, Gitlin JD. Coordination of development and metabolism in the pre-midblastula transition zebrafish embryo. Dev Dyn 2008a;237:1789–1798. [PubMed: 18521947]

Mendelsohn BA, Kassebaum BL, Gitlin JD. The zebrafish embryo as a dynamic model of anoxia tolerance. Dev Dyn 2008b;237:1780–1788. [PubMed: 18521954]

Ono S, Ono K. Tropomyosin inhibits ADF/cofilin-dependent actin filament dynamics. J Cell Biol 2002;156:1065–1076. [PubMed: 11901171]

Owen CH, DeRosier DJ, Condeelis J. Actin crosslinking protein EF-1a of Dictyostelium discoideum has a unique bonding rule that allows square-packed bundles. J Struct Biol 1992;109:248–254. [PubMed: 1296758]

Padilla PA, Roth MB. Oxygen deprivation causes suspended animation in the zebrafish embryo. Proc Natl Acad Sci USA 2001;98:7331–7335. [PubMed: 11404478]

Scandurro AB, Weldon CW, Figueroa YG, Alam J, Beckman BS. Gene microarray analysis reveals a novel hypoxia signal transduction pathway in human hepatocellular carcinoma cells. Int J Oncol 2001;19:129–135. [PubMed: 11408933]

Schwartz N, Hosford M, Sandoval RM, Wagner MC, Atkinson SJ, Bamburg J, Molitoris BA. Ischemia activates actin depolymerizing factor: role in proximal tubule microvillar actin alterations. Am J Physiol 1999;276:F544–551. [PubMed: 10198413]

Shakib K, Norman JT, Fine LG, Brown LR, Godovac-Zimmermann J. Proteomics profiling of nuclear proteins for kidney fibroblasts suggests hypoxia, meiosis, and cancer may meet in the nucleus. Proteomics 2005;5:2819–2838. [PubMed: 15942958]

Son D, Kojima I, Inagi R, Matsumoto M, Fujita T, Nangaku M. Chronic hypoxia aggravates renal injury via suppression of Cu/Zn-SOD: a proteomic analysis. Am J Physiol Renal Physiol 2008;294:F62–72. [PubMed: 17959751]

St-Pierre J, Brand MD, Boutilier RG. Mitochondria as ATP consumers: cellular treason in anoxia. Proc Natl Acad Sci USA 2000;97:8670–8674. [PubMed: 10890886]

Storey KB. Gene hunting in hypoxia and exercise. Adv Exp Med Biol 2006;588:293–309. [PubMed: 17089897]

Suurna MV, Ashworth SL, Hosford M, Sandoval RM, Wean SE, Shah BM, Bamburg JR, Molitoris BA. Cofilin mediates ATP depletion-induced endothelial cell actin alterations. Am J Physiol 2006;290:F1398–1407.

Tay TL, Lin Q, Seow TK, Tan KH, Hew CL, Gong Z. Proteomic analysis of protein profiles during early development of the zebrafish, Danio rerio. Proteomics 2006;6:3176–3188. [PubMed: 16622891]

Thisse, B.; Thisse, C. Fast Release Clones: A High Throughput Expression Analysis. ZFIN Direct Data Submission. 2004. http://zfin.org

Tonge R, Shaw J, Middleton B, Rowlinson R, Rayner S, Young J, Pognan F, Hawkins E, Currie I, Davison M. Validation and development of fluorescence two-dimensional differential gel electrophoresis proteomics technology. Proteomics 2001;1:377–396. [PubMed: 11680884]

Ünlü M, Morgan ME, Minden JS. Difference gel electrophoresis: a single gel method for detecting changes in protein extracts. Electrophoresis 1997;18:2071–2077. [PubMed: 9420172]

van Rheenen J, Song X, van Roosmalen W, Cammer M, Chen X, Desmarais V, Yip SC, Backer JM, Eddy RJ, Condeelis JS. EGF-induced PIP2 hydrolysis releases and activates cofilin locally in carcinoma cells. J Cell Biol 2007;179:1247–1259. [PubMed: 18086920]

Vayda ME, Shewmaker CK, Morelli JK. Translational arrest in hypoxic potato tubers is correlated with the aberrant association of elongation factor EF-1 alpha with polysomes. Plant Mol Biol 1995;28:751–757. [PubMed: 7647305]

Wulff T, Hoffmann EK, Roepstorff P, Jessen F. Comparison of two anoxia models in rainbow trout cells by a 2-DE and MS/MS-based proteome approach. Proteomics 2008a;8:2035–2044. [PubMed: 18491317]

Wulff T, Jessen F, Roepstorff P, Hoffmann EK. Long term anoxia in rainbow trout investigated by 2-DE and MS/MS. Proteomics 2008b;8:1009–1018. [PubMed: 18240135]

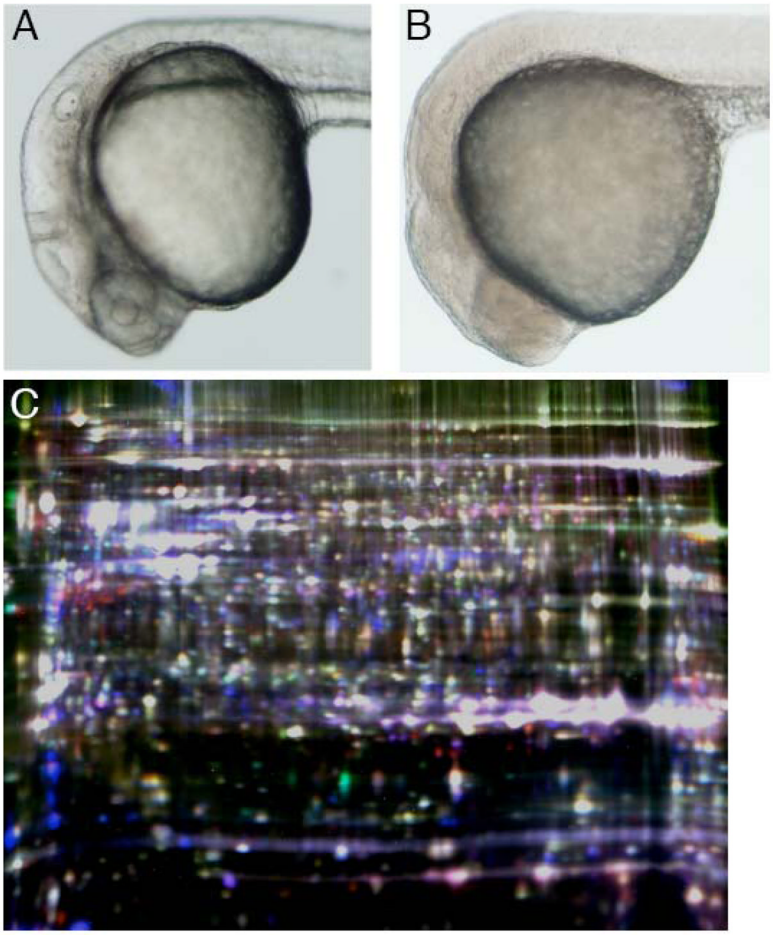

Fig. 1.

Appearance of normoxic and anoxic zebrafish embryos. (A) Normoxic embryo at 24 hpf and (B) 24 hpf embryo after an additional 24 h of anoxia. (C) Two-dimensional gel of proteins labeled with cyanine dyes from zebrafish embryos at 24 hpf normoxic (Cy2), 48 hpf normoxic (Cy3) and 24 hpf + 24 h anoxia (Cy5) (Gel 3).

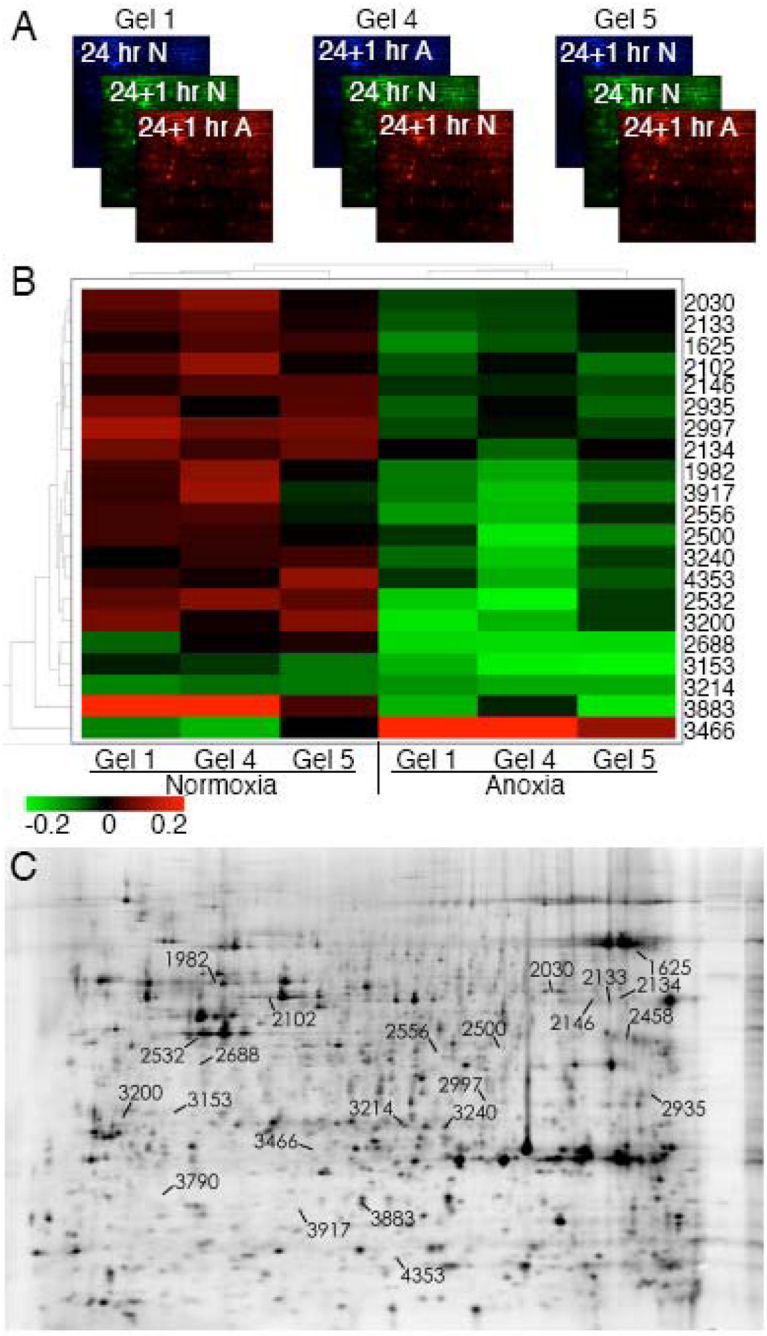

Fig. 2.

2D-DIGE analysis of proteomic changes induced by acute anoxia using an internal standard. (A) Schematic of experimental design in which three 2D gels were run with lysates from 24 hpf embryos using the 24 hpf, normoxic sample as the internal standard (Cy2, Cy3, Cy3 in gels 1, 4, and 5 respectively), and comparing 24 hpf + 1 h normoxia (Cy3, Cy5, Cy2) with 24 hpf + 1 h anoxia (Cy5, Cy2, Cy5). (B) Heat map analysis of statistically significant ($p<0.05$) proteomic changes after 1 h of anoxia. The color in each panel represents the relative change compared to the internal standard (24 hpf, normoxic) in each individual gel. (C) Image of Gel 4 indicating the location of the spots comprising the heat map.

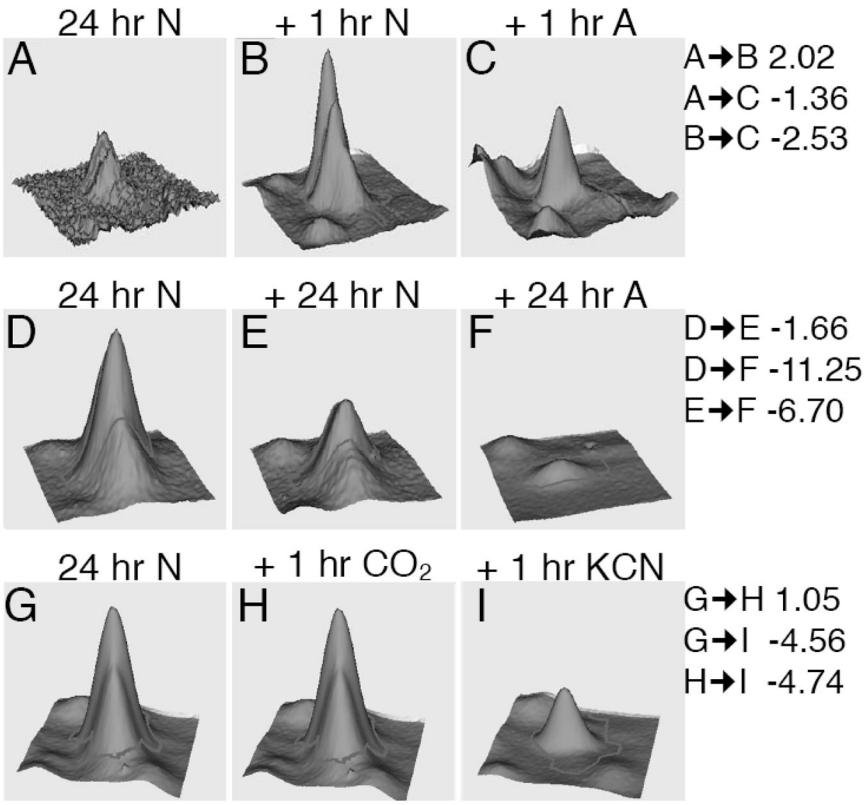

Fig. 3.

Analysis of cofilin changes in acute and prolonged anoxia, and in CO_2 and KCN. (A–C) 3D quantitative representation of a spot determined to represent muscle cofilin 2 at 24 hpf, 24 + 1 h normoxia and 24 + 1 h anoxia. (D–F) Cofilin abundance in the same spot at 24 hpf, 24 + 24 h normoxia and 24 +24 h anoxia. (G–I) Cofilin abundance in 24 hpf embryos compared to 24 + 1 h in 5% CO_2 or 1 h in 500 μM KCN. Fold changes between each sample are indicated on the right.

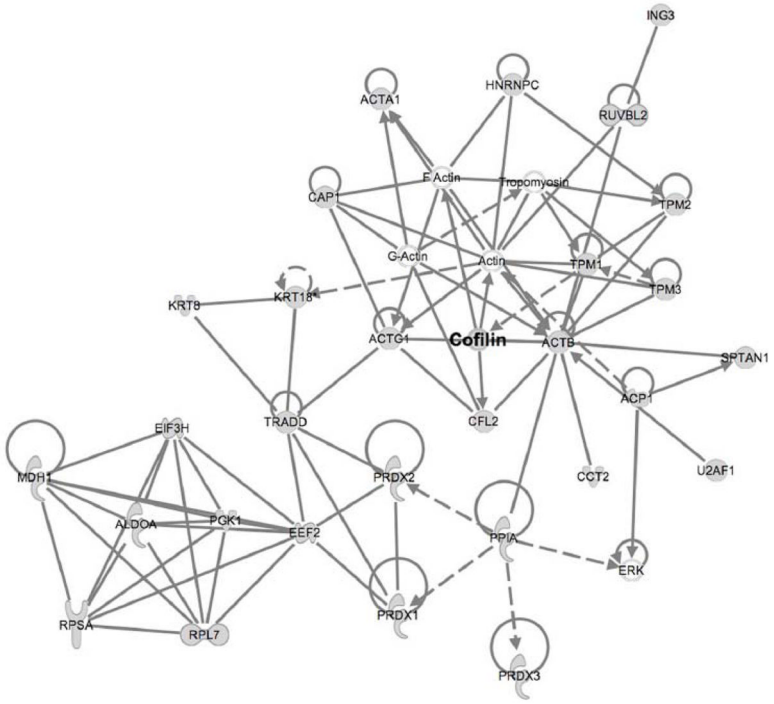

Fig. 4.

Pathways associated with proteins identified by 2D-DIGE as changing in acute or prolonged anoxia. Ingenuity Pathway Analysis software (Ingenuity Systems, Inc.) was utilized to map proteins identified onto existing pathways that are based on established interactions. Shading indicates proteins identified by 2D-DIGE/MS, while unshaded proteins represent components of these pathways not detected by 2D-DIGE/MS. The full name of each protein is given in Table S3.

Table 1

Identified proteins changing after 1 h in anoxia (Gel 1).

Spot ID	Protein identification	Protein accession number	Est. % coverage	Spectral count	24N > +1hN	Fold Change[1] 24N > +1hA	25N > +24hA
3216					**−1.08**	**−1.64**	**−1.54**
	Krt4 protein	gi|44890667	64%	96			
	desmin	gi|18858539	47%	26			
3246					**1.08**	**1.94**	**1.77**
	elongation factor 1-alpha	gi|18858587	36%	26			
	vitellogenin 5	gi|68448530	18%	13			
	vitellogenin 1	gi|25092674	9%	13			
3247					**1.12**	**2.27**	**2.01**
	elongation factor 1-alpha	gi|18858587	51%	23			
	Vitellogenin 5	gi|68448530	13%	12			
	vitellogenin 1	gi|25092674	17%	14			
	mitochondrial ATP synthase alpha subunit	gi|44969408	5%	2			
3532					**−1.08**	**−1.56**	**−1.47**
	Ubiquinol-cytochrome c reductase core protein II	gi|50540382	17%	6			
	creatine kinase	gi|125837832	22%	8			
	S-adenosylhomocysteine hydrolase	gi|40363541	19%	4			
	creatine kinase, muscle	gi|18858427	19%	7			
	acyl-Coenzyme A dehydrogenase, long chain	gi|41056265	21%	9			
	vitellogenin 1	gi|25092674	8%	5			
3847					**1.42**	**2.01**	**1.4**
	eukaryotic translation elongation factor 2, like	gi|41386743	14%	30			
	enolase 3, (beta, muscle)	gi|47551317	17%	7			
	hypothetical protein LOC550494	gi|62955565	14%	4			
	v-crk sarcoma virus CT10 oncogene homolog (avian)-like	gi|47087217	9%	2			
	eukaryotic translation initiation factor 3, subunit 3	gi|57768898	8%	3			
	myosin, heavy polypeptide 2, fast muscle specific	gi|50512294	7%	2			
	CHORD-containing, zinc binding protein 1	gi|41056073	9%	3			
4252					**−1.12**	**−1.69**	**−1.52**

Spot ID	Protein identification	Protein accession number	Est. % coverage	Spectral count	24N > +1hN	Fold Change[1] 24N > +1hA	25N > +24hA
	vitellogenin 1	gi|25092674	11%	25			
	esterase D/formylglutathione hydrolase	gi|68448530	9%	23			
	annexin A4	gi|32401412	41%	13			
4557					**−1.28**	**−1.94**	**−1.54**
	esterase D/formylglutathione hydrolase	gi|68448530	10%	19			
	vitellogenin 6	gi|57864787	35%	15			
	vitellogenin 4	gi|57864783	38%	11			
4604					**−1.11**	**−2.23**	**−2.04**
	beta-tubulin	gi|41053911	12%	5			
	thioredoxin family Trp26	gi|46309519	20%	3			
	capping protein (actin filament) muscle Z-line, beta	gi|41053959	8%	2			
4615					**1.14**	**−1.47**	**−1.69**
	vitellogenin 1	gi|25092674	21%	36			
	esterase D/formylglutathione hydrolase	gi|68448530	21%	34			
	proteasome subunit beta 7	gi|5833465	51%	26			
	proteasome 26S non-ATPase subunit 8	gi|50344918	53%	14			
	Eukaryotic translation elongation factor 2, like	gi|28278942	8%	14			
4637					**−1.16**	**−2.31**	**−2.01**
	vitellogenin 1	gi|25092674	13%	27			
	proteasome 26S non-ATPase subunit 11	gi|68437953	12%	5			
	vitellogenin 3 precursor	gi|11118642	2%	3			
	similar to cytokine-like nuclear factor n-pac isoform 3	gi|56090178	9%	3			
	hydroxysteroid dehydrogenase like 2	gi|37589816	19%	2			
5131					**1.07**	**1.59**	**1.46**
	peroxiredoxin 2	gi|50539996	78%	17			
	ferritin, heavy polypeptide 1	gi|18858719	23%	5			
5215					**1.72**	**−1.48**	**−2.58**
	phospholipid hydroperoxide glutathione peroxidase B	gi|29648610	70%	14			
	esterase D/formylglutathione hydrolase	gi|68448530	5%	2			
5317					**1.51**	**−1.71**	**−2.62**
	Setb protein	gi|42542468	17%	4			

Spot ID	Protein identification	Protein accession number	Est. % coverage	Spectral count	24N > +1hN	Fold Change[1] 24N > +1hA	25N > +24hA
	ribosomal protein L11	gi|50344934	16%	3			
	ADP-ribosylation factor 5	gi|40548312	11%	2			
	Taldo1 protein	gi|45786121	6%	2			
5298					**−1.05**	**−3.52**	**−3.39**
	ribosomal protein SA	gi|41054972	30%	7			
	muscle cofilin 2	gi|47271384	20%	3			
5183					**−3.42**	**1.54**	**5.21**
	glia maturation factor beta	gi|47085855	37%	4			
5297					**1.04**	**−2.31**	**−2.45**
	muscle cofilin 2	gi|47271384	37%	8			
	vitellogenin 1	gi|25092674	5%	4			
5484					**1.44**	**−1.87**	**−2.72**
	acid phosphatase 1	gi|62122785	45%	10			
	similar to Stathmin (Phosphoprotein p19)	gi|68431633	18%	3			
	Krt4 protein	gi|44890667	19%	2			

[1]The difference in spot volumes for each pairwise comparison is indicated by a positive or negative value for an increase or decrease, respectively, from the first to the second condition in each comparison.

Table 2

Distribution of spots by fold change after 24 h in anoxia.

Fold change	# spots	% total
>10	3	0.07
5 to 10	7	0.16
2 to 5	205	4.57
1.5 to 2	530	11.80
1 to 1.5	3745	83.41

Table 3

Analysis of proteins changing after 24 h in anoxia (Gel 2).

Spot ID	Protein identification	Protein accession number	Est. % coverage	Spectral count	24N > +6hN	Fold Change 24N > +24hA	30N > +24hA
2121					**1.09**	**3.08**	**2.81**
	vitellogenin 1	gi|25092674	15%	18			
	similar to Filamin A	gi|68402025	4%	8			
2652					**1.10**	**3.60**	**3.26**
	tubulin, beta 2c	gi|47087299	30%	16			
	Heat shock protein 8	gi|28279108	16%	10			
3054					**1.28**	**3.04**	**2.36**
	keratin	gi|62955153	46%	14			
	DEAD/H box polypeptide 19	gi|27881976	17%	6			
3955					**−1.25**	**−3.53**	**−2.84**
	vitellogenin 2	gi|68400037	14%	16			
	vitellogenin 1	gi|25092674	12%	14			
	vitellogenin 5	gi|68448530	19%	15			
	cytosolic malate dehydrogenase A	gi|29242793	19%	4			
	similar to cathepsin L isoform 3	gi|68369812	34%	5			
	similar to cathepsin L isoform 2	gi|68369848	32%	5			
4161					**−1.50**	**−4.11**	**−2.76**
	similar to vitellogenin	gi|68400037	7%	12			
	vitellogenin 1	gi|25092674	6%	8			
4172					**−1.40**	**−6.95**	**−5.00**
	vitellogenin 1	gi|25092674	12%	14			
	vitellogenin 2	gi|68400037	13%	16			
	vitellogenin 5	gi|68448530	10%	15			
4569					**−1.24**	**−5.16**	**−4.20**
	similar to vitellogenin	gi|68400037	8%	14			
	vitellogenin 1	gi|25092674	8%	11			
	pyrroline-5-carboxylate reductase-like	gi|66472516	16%	3			
4716					**−1.45**	**−3.11**	**−2.15**
	vitellogenin 5	gi|68448530	19%	13			

Spot ID	Protein identification	Protein accession number	Est. % coverage	Spectral count	24N > +6hN	Fold Change 24N > +24hA	30N > +24hA
	vitellogenin 2	gi|68400037	11%	13			
	vitellogenin 1	gi|25092674	19%	12			
	mitochondrial ATP synthase alpha subunit	gi|44969408	26%	2			
	dodecenoyl-Coenzyme A delta isomerase	gi|32766683	12%	3			
	electron-transfer-flavoprotein	gi|47085679	28%	3			
	proteasome subunit alpha type 7	gi|47085943	8%	2			
4910					**−1.45**	**−3.02**	**−2.09**
	similar to vitellogenin	gi|68400037	6%	9			
	vitellogenin 5	gi|68448530	4%	6			
	vitellogenin 1	gi|25092674	5%	6			
5244					**−1.34**	**−3.20**	**−2.41**
	vitellogenin 1	gi|25092674	11%	7			
5563					**1.47**	**−5.02**	**−7.40**
	ribosomal protein SA	gi|41054972	21%	5			
	muscle cofilin 2	gi|47271384	15%	2			
5825					**−1.12**	**−4.03**	**−3.62**
	RNA pol II transcriptional coactivator PC4	gi|50540080	16%	3			
5931					**1.58**	**10.10**	**6.34**
	RNA pol II transcriptional coactivator PC4	gi|50540080	28%	4			
6703					**−1.51**	**−3.22**	**−2.14**
	S100 calcium binding protein A1	gi|68384208	60%	3			
	vitellogenin 5	gi|68448530	10%	2			

Table 4

Analysis of proteins changing after prolonged anoxia (Gel 3).

Spot ID	Protein identification	Protein accession number	Est. % coverage	Spectral count	24N > +24hN	Fold Change 24N > +24hA	48N > +24hA
1333					**1.01**	**4.13**	**4.15**
	spectrin alpha 2	gi|62203376	19%	4			
	Krt4 protein	gi|44890667	8%	3			
3267					**1.41**	**3.54**	**2.54**
	annexin A11b	gi|32401408	22%	7			
	serine hydroxymethyltransferase 1 (soluble)	gi|41054918	14%	7			
	CAP, adenylate cyclase-associated protein 1	gi|41054003	8%	4			
	mitochondrial ATP synthase alpha subunit	gi|44969408	6%	2			
3453					**−2.92**	**2.41**	**7.13**
	elongation factor 1-alpha	gi|18858587	26%	15			
	vitellogenin 5	gi|68448530	7%	4			
3845					**4.19**	**−2.25**	**−9.36**
	Krt4 protein	gi|44890667	51%	49			
	Suclg2 protein	gi|33989739	33%	12			
	alpha-cardiac actin	gi|6636384	19%	8			
	bactin1	gi|18858335	16%	6			
3917					**1.08**	**−2.39**	**−2.55**
	similar to RNA binding motif protein 4	gi|47086959	58%	31			
	vitellogenin 5	gi|68448530	12%	12			
	similar to vitellogenin	gi|68400037	5%	8			
	Aldolase b, fructose-bisphosphate	gi|29477118	27%	5			
	glutamate oxaloacetate transaminase 2	gi|41053395	7%	3			
	aldolase A	gi|22671688	15%	5			
3983					**−1.48**	**2.41**	**3.61**
	similar to cathepsin L isoform 2	gi|68369808	25%	5			
	annexin A4	gi|32401412	14%	5			
	dihydrodiol dehydrogenase	gi|53933262	8%	2			
4091					**−2.07**	**2.77**	**5.81**

Spot ID	Protein identification	Protein accession number	Est. % coverage	Spectral count	24N > +24hN	Fold Change 24N > +24hA	48N > +24hA
	Krt4 protein	gi|44890667	49%	32			
	keratin 18	gi|29335504	61%	29			
	cathepsin D	gi|18858489	21%	7			
	heterogeneous nuclear ribonucleoprotein C	gi|47085809	21%	9			
	ubiquitin carboxyl-terminal hydrolase	gi|47085817	16%	6			
4124					**2.45**	**3.02**	**1.24**
	tropomyosin 2 (beta)	gi|50344894	52%	22			
	alpha-tropomyosin	gi|18859505	34%	16			
	nucleophosmin 1	gi|40786521	18%	3			
	signal sequence receptor, alpha	gi|41151978	8%	2			
	Krt4 protein	gi|44890667	11%	2			
	keratin 18	gi|29335504	35%	2			
4153					**1.51**	**3.44**	**2.31**
	Krt4 protein	gi|44890667	43%	26			
	proteasome (prosome, macropain) 26S subunit, ATPase, 3	gi|50344782	14%	11			
4180					**1.13**	**4.37**	**3.90**
	Krt4 protein	gi|44890667	45%	28			
	keratin 18	gi|29335504	32%	15			
	heterogeneous nuclear ribonucleoprotein C	gi|47085809	19%	7			
4242					**−1.48**	**−5.22**	**−3.50**
	nascent polypeptide-associated complex alpha polypeptide	gi|27545279	33%	7			
4253					**1.47**	**6.86**	**4.71**
	Krt4 protein	gi|44890667	39%	21			
	alpha-tropomyosin	gi|18859505	21%	5			
4464					**−1.05**	**2.31**	**2.44**
	nascent polypeptide-associated complex alpha polypeptide	gi|27545279	24%	3			
4568					**−1.23**	**2.24**	**2.78**
	splicing factor, arginine/serine-rich 2	gi|47087067	20%	4			
	OTU domain, ubiquitin aldehyde binding 1, like	gi|50539890	8%	2			
5427					**−1.69**	**4.27**	**7.31**
	peroxiredoxin 1	gi|61806512	33%	8			

Spot ID	Protein identification	Protein accession number	Est. % coverage	Spectral count	24N > +24hN	Fold Change 24N > +24hA	48N > +24hA
	vitellogenin 1	gi|25092674	7%	6			
	proteasome (prosome, macropain) subunit, beta type, 2	gi|50540284	25%	9			
	splicing factor, arginine/serine-rich 3 isoform 2	gi|41151986	25%	4			
5531					**1.47**	**3.18**	**4.61**
	vitellogenin 5	gi|68448530	10%	4			
5665					**1.48**	**4.71**	**3.21**
	tyrosine 3-monooxygenase/tryptophan 5-monooxygenase activation protein, beta polypeptide like	gi|41152453	9%	2			
5807					**−1.66**	**−11.25**	**−6.70**
	muscle cofilin 2	gi|47271384	26%	3			
	basic transcription factor 3-like 4	gi|41152344	5%	2			
6006					**1.57**	**−2.29**	**−3.56**
	ADP-ribosylation factor 1	gi|41393073	17%	3			
6108					**1.43**	**−2.36**	**−3.35**
	troponin C, fast skeletal	gi|18859495	25%	3			
	calmodulin 2 [Homo sapiens]	gi|4502549	44%	5			

Table 5

BVA analysis of proteins changing after acute anoxia (picked from Gel 4).

Spot ID	Protein identification	Protein accession number	Est. % coverage	Spectral count	t-test	Average fold change 25N > +1hA
1625					0.03	**−1.21**
	decapentaplegic and Vg-related 1	gi|18858571	19%	3		
1982					0.02	**−1.35**
	keratin 8	gi|41056085	42%	26		
	Krt4 protein	gi|44890667	13%	7		
2030					0.044	**−1.20**
	mitochondrial ATP synthase alpha subunit	gi|44969408	44%	18		
2102					0.043	**−1.26**
	Krt4 protein	gi|44890667	47%	27		
	RuvB-like 2	gi|27819634	20%	6		
2133					0.034	**−1.17**
	elongation factor 1-alpha	gi|18858587	21%	9		
2134					0.042	**−1.19**
	elongation factor 1-alpha	gi|18858587	20%	13		
	vitellogenin 5	gi|68448530	6%	2		
2146					0.004	**−1.18**
	elongation factor 1-alpha	gi|18858587	16%	7		
2458					0.027	**−1.29**
	Aldolase b, fructose-bisphosphate	gi|29477118	12%	3		
	vitellogenin 5	gi|57864785	6%	2		
	aldolase A	gi|22671688	10%	3		
2532					0.017	**−1.56**
	Krt4 protein	gi|44890667	26%	10		
	Bactin1 protein	gi|28279111	30%	8		
	actin, alpha 1, skeletal muscle	gi|18858249	23%	7		
3200					0.023	**−1.49**
	tropomyosin 3	gi|41393141	28%	5		
	type I cytokeratin, enveloping layer	gi|18858519	25%	3		
	apolipoprotein Eb	gi|18858283	7%	2		

Spot ID	Protein identification	Protein accession number	Est. % coverage	Spectral count	t-test	Average fold change 25N > +1hA
3214					0.016	**−1.09**
	vitellogenin 5	gi|57864785	21%	6		
	phosphoglycerate mutase 1	gi|38488700	14%	4		
3790					0.041	**1.50**
	type II cytokeratin	gi|18858425	3%	2		
3883					0.029	**−2.12**
	muscle cofilin 2	gi|47271384	49%	10		